ACS chemical biology

Reviews

Cite This: ACS Chem. Biol. 2019, 14, 2102−2114

pubs.acs.org/acschemicalbiology

# Specific Recognition of Promoter G-Quadruplex DNAs by Small Molecule Ligands and Light-up Probes

V. Dhamodharan*,†,‡ and P. I. Pradeepkumar*,†

†Department of Chemistry, Indian Institute of Technology Bombay, Mumbai 400076, India

‡Okinawa Institute of Science and Technology Graduate University, Okinawa 9040495, Japan

**ABSTRACT:** G-Quadruplexes (G4s) are four-stranded nucleic acid structures whose underlying G-rich sequences are present across the chromosome and transcriptome. These highly structured elements are known to regulate many key biological functions such as replication, transcription, translation, and genomic stability, thereby providing an additional layer of gene regulation. G4s are structurally dynamic and diverse, and they can fold into numerous topologies. They are potential targets for small molecules, which can modulate their functions. To this end, myriad classes of small molecules have been developed and studied for their ability to bind and stabilize these unique structures. Though many of them can selectively target G4s over duplex DNA, only a few of them can distinguish one G4 topology from others. Design and development of G4-specific ligands are challenging owing to the subtle structural variations among G4 structures. However, screening assays and computational methods have identified a few classes of ligands that preferentially or specifically target the G4 topology of interest over others. This review focuses on the small molecules and fluorescent probes that specifically target human promoter G4s associated with oncogenes. Targeting promoter G4s could circumvent the issues such as undruggability and development of drug resistance associated with the protein targets. The ligands discussed here highlight that development of G4-specific ligands is an achievable goal in spite of the limited structural data available. The future goal is to pursue the development of G4-specific ligands endowed with drug-like properties for G4-based therapeutics and diagnostics.

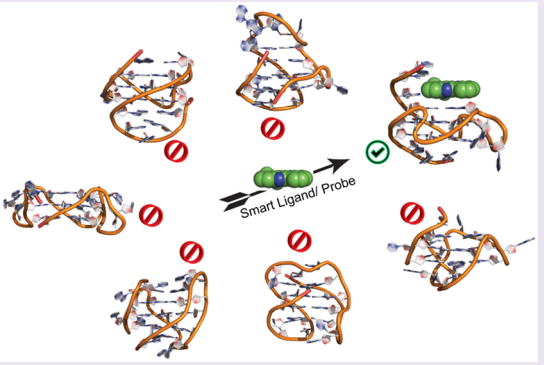


## INTRODUCTION

Certain G-rich nucleic acid sequences are capable of folding into four-stranded structures called G-quadruplexes (G4s), which are formed by the stacking of two or more G-quartets in the presence of metal ions such as $K^+$ and $Na^+$ (Figure 1).[1] G4s adopt various structural topologies such as parallel, antiparallel, and mixed-type (hybrid) with right-handed helicity, depending on the nature and length of the loops, flanking sequences, nature of metal ions, and environmental conditions. The structural space and complexity are more likely to broaden with the recent finding of a left-handed G4 motif.[2] A high-throughput sequencing method, G4-seq, identified 716 310 potential G4 forming sequences in the human genome, which vastly exceeds the number of sequences, ∼370 000, predicted by the computational algorithms that had not considered the long loop (>7 nt) and bulges in the strands.[3] However, only ∼10 000 endogenous G4 structures have been identified within the context of human chromatin by the G4-ChIP-seq.[4] G4 structures have been visualized at the telomere, across the chromosome, and in the transcriptome by using G4-specific antibodies and fluorescent ligands.[5−9]

G4s are known to play critical roles in fundamental cellular functions such as telomere maintenance, replication, genome stability, transcription, and translation.[10] They can impede the replication and are the source of genome instability when the G4 helicase activities are impaired.[11,12] Telomeric G4 interferes with the function of telomerase, whereas promoter G4s regulate transcription.[13] The RNA G4s located in 5′-UTRs (UTRs = untranslated regions) modulate translation in both cap-dependent and cap-independent mechanisms, while those located in the certain 3′-UTRs involved in the alternative polyadenylation and regulation of micro RNAs.[14−16] Also, several cellular proteins including nucleolin, PARP1, and FMR2 bind to G4s; various helicases such as Pif1, RecQ, FANCJ, WRN, BLM, and RHAU unfold the G4s, underscoring a myriad number of roles played by these structures.[17,18]

G4s are highly dynamic and readily fold under the physiological condition *in vitro*.[1] Formation of G4s in the chromatin and transiently folded RNA G4s in the transcriptome have been observed, which can be targeted and stabilized by an exogenous small molecule.[4,27] G4s are therapeutic targets for small molecules that induce double-strand breaks (DSB), DNA damage response, and synthetic lethality in cancer cells.[28−31] G4s are also potential targets for neurodegenerative diseases.[32] Interestingly, two G4 binding

Received: June 16, 2019
Accepted: September 18, 2019
Published: September 18, 2019






DOI: 10.1021/acschembio.9b00475
ACS Chem. Biol. 2019, 14, 2102−2114

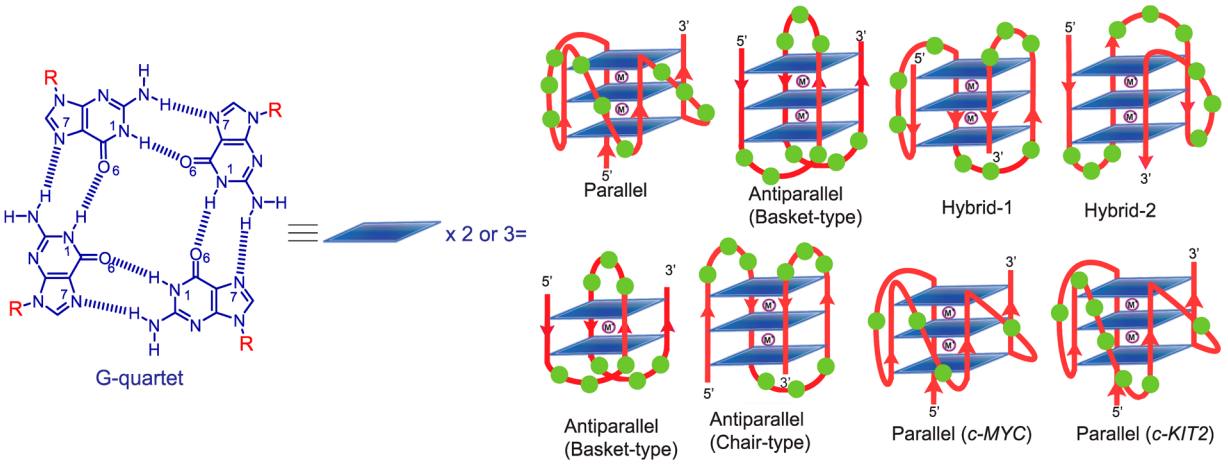


**Figure 1.** Schematic representation of G-quartet and representative topologies of telomeric and promoter G4s. G-Quartet, also known as G-tetrad, formed by the self-association of four guanine bases through Hoogsteen hydrogen bonding; stacks of two or more quartets result in folding of G4s, which are stabilized by monovalent metal ions ($M^+$). The nucleotides that constitute the loops are shown in the green sphere. Loops are categorized into three different types, namely, diagonal, lateral, and chain reversal (propeller). Telomeric G4s: parallel (PDB: 1KF1),[19] basket-type antiparallel (PDB: 143D),[20] hybrid-1 (PDB: 2GKU),[21] hybrid-2 (PDB: 2JPZ),[22] 2-quartet basket type antiparallel (PDB: 2KF8)[23] and chair-type antiparallel (PDB: 5YEY).[24] Promoter G4s: *c-MYC* (PDB: 1XAV)[25] and *c-KIT2* (PDB: 2KQH).[26] The parallel G4 strands are connected via three propeller loops, whereas antiparallel ones are connected through two lateral and one diagonal loops, and hybrid G4s have two lateral and one propeller loops.

small molecules, quarfloxin (CX-3543) and CX-5461, reached the clinal trial for the treatment of cancer.[30,33] CX-5461 is directed toward breast cancer tumor suppressor genes (BRCA1/2) deficient tumors, while CX-3543 was terminated in Phase II due to its bioavailability issue.[30,33] Moreover, findings of G4 structures in virus, bacteria, and parasites open up avenues for targeting them with small molecules, highlighting their importance in human health.[34,35]

**Structure and Function of G4s.** Telomeric G4 DNA is highly polymorphic and is known to adopt various G4 topologies (Figure 1). The 22nt human telomeric DNA, $AG_3(T_2AG_3)_3$, adopts antiparallel topology under $Na^+$ ions, but the same sequence crystallized into the parallel form in the presence of $K^+$ ions.[19,20] Depending on the particular flanking nucleotides, multiple G4 topologies such as hybrid-1, hybrid-2, and 2-tetrad antiparallel G4s have been reported for the telomeric DNA (Figure 1).[1] In the presence of crowding agents such as poly(ethylene glycol) (PEG), telomeric G4 adopts parallel form owing to conformational selection and dehydrating effect of PEG.[36,37] However, when *Xenopus laevis* egg extract was used as a crowding agent, the hybrid-1, hybrid-2, and 2-quartet antiparallel G4s (Figure 1) were found to be the only biologically relevant conformations,[38,39] which were also observed in living human cells.[40] Formation of higher-order G4s (tandem G4s)[41] further complicates the relevant conformation needed for the ligand design and screening.

The promoter regions of proto-oncogenes such as *c-MYC*, *c-KIT*, *BCL-2*,*VEGF*, *SRC*, *hTERT*, *RET*, *PDGFR-β*, *PDGF-A*, *KRAS*, *HRAS*, *HIF-1α*, and *c-MYB* contain G-rich sequences, which have a propensity to form stable G4 structures.[33] The negative superhelicity induced by transcription and molecular crowding conditions favor the formation of the G4 structure in G-rich strands and the i-motif in the C-rich strands from the corresponding duplex DNA.[42,43] The concurrent or mutually exclusive formation of G4 and i-motif from corresponding duplex sequence depends on the distance between the two secondary structures.[44,45] The dynamic G4 structure can be stabilized by a small molecule ligand, and thus the resulting stable G4 poses a challenge to transcription machinery, which results in repression of the associated gene expression (Figure 2).[46] One of the most studied promoter G4s is *c-MYC*, whose

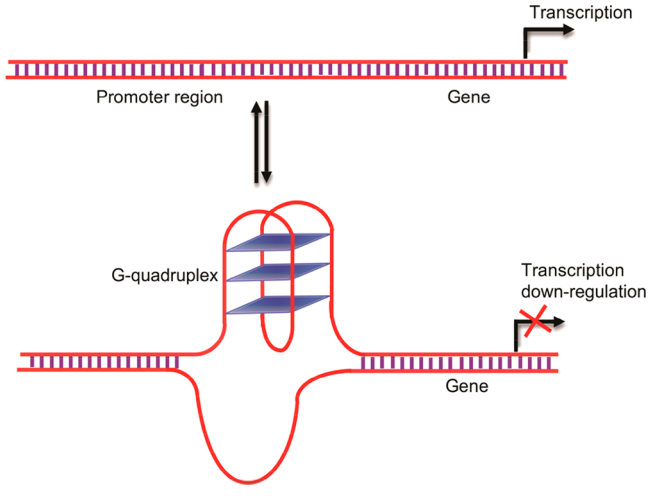


**Figure 2.** Proposed transcriptional regulation of promoter G4s. Transcriptionally induced negative superhelicity, G4-associated proteins, and molecular crowding are likely to favor the formation of secondary structures.

overexpression leads to ~80% of all solid tumors, including medulloblastomas, breast, ovarian, and gastrointestinal cancers.[33,47] The nuclease hypersensitive element (NHE) $III_1$ that is critical for regulating *c-MYC* expression comprises a 27-nt G4 forming sequence from −115 to −142 bp upstream of the transcription start site.[25] MYC protein constitutes an "undruggable" target, because it is an intrinsically disordered protein that lacks a defined enzymatic site or binding pocket, and thus it is not amenable to small-molecule inhibition.[48] In this context, *c-MYC* G4 provides an attractive target for small molecules to regulate its expression.[47] An exon-specific assay involving CA46 cells has been used to validate whether ligand-


DOI: 10.1021/acschembio.9b00475
ACS Chem. Biol. 2019, 14, 2102−2114

induced downregulation of the c-*MYC* mRNA expression is directly mediated via targeting corresponding G4 or not.[49,50]

*c-KIT* is another proto-oncogene, which encodes for a tyrosine kinase receptor. Two G4 forming sequences, namely, *KIT1* (from −87 to −109 bp) and *KIT2* (from −140 to −160 bp) are located in the upstream of transcriptional start site of *KIT* gene.[51,52] Mutation and overexpression of c-KIT protein is associated with gastrointestinal stromal tumors (GISTs) and the mesenchymal tumors of the stomach and proximal small intestine.[53] Drug resistance issue associated with the small molecules targeting c-KIT protein warrants *c-KIT* G4s to be considered an alternative way to regulate its expression by small molecules.[54] Structural analysis of promoter G4s indicates that most of G4s such as *c-MYC*, *c-KIT*, *VEGF*, *RET*, and *HIF-1α* comprise single-nucleotide loops (first and third) and a loop having variable length in the middle; the short loop-size favors the parallel topology (Figure 1).[55,56] Other promoter G4s such as *BCL-2* and *hTERT* fold into hybrid forms, besides parallel forms.[55,57,58]

G4 formation at the 5′-UTRs of many genes such as *NRAS*, *ZIC1*, *MT3-MM3*, *BCL-2*, and *ERS1* is known to repress the translation process, whereas G4 formation at 5′-UTRs of *FGF-2* and *VEGF* promotes the translation.[14] Furthermore, the G-rich telomeric repeat-containing RNA (TERRA) is known to fold into a parallel G4 structure.[1] Formation of G4s has also been reported near the rRNA (ribosomal RNA) tentacles.[59] Unlike structural diversity of DNA G4s, RNA G4s are mostly known to fold into the parallel topology, with the exception of recent finding suggesting the formation of antiparallel G4 RNA.[60] Because of the steric constraint imposed by 2′-OH group, the ribose sugars favor mostly the anticonformation of the glycosidic bond, which in turn leads to the parallel topology. There also exist conformational dynamics between a hairpin and G4 for some G-rich RNAs.[61] Despite a recent finding suggesting that RNA G4s are globally unfolded *in vivo*,[62] small molecule based high-throughput sequencing (G4RP-seq) identifies *in vivo* existence of transiently folded RNA G4s in the transcriptome.[27]

**Specific Targeting of G4s.** G4-Specific ligands and fluorescent probes are warranted at least for the following reasons: (1) indiscriminate and stochastic binding to all G4 may lead to breaks in replication fork and can induce genome instability,[63−65] (2) to understand the formation and function of G4s of interest in the genome, (3) G4-specific therapeutic intervention to alleviate off-target toxicity, (4) locus-specific visualization and identification of G4s, and (5) to find out whether the G4 of interest is folded or not in both *in vitro* and *in vivo* conditions. The focus of the review is to highlight the limited success achieved in the design and development of ligands that stabilize promoter G4s specifically over related G4s and duplex DNAs. Besides, the probes that sense the promoter G4s selectively through their fluorescence light-up are discussed.

A number of ligands targeting G4 structures with superior selectivity over the duplex DNA have been reported.[31,54,66−69]However, specificity toward a G4 of interest over other structurally similar G4s is a challenging task given their subtle structural variations in loops (length, composition, and type), groove widths (narrow, medium, and wide), and flanking nucleotides.[70] This is further complicated by the ligand-induced fit that alters the loop conformation, groove dimension, and flanking nucleotide arrangement and by the conformational selection that transduces the polymorphic G4s into a ligand-favored topology.[36,68,71,72] Though a limited number of small molecules have shown specific binding preference for a particular G4 over others,[73−81] the fundamental question remains whether the challenge of designing such molecules is worth pursuing given that complex diseases such as cancer involve intricately multiple pathways and genes.[82] On the one hand, even if the ligands are specific toward a particular type of G4s, screening against the overwhelmingly available structurally related G4s is a daunting task. On the other hand, whether all the potential G4 forming sequences can fold into G4s in cells is unclear, as it depends on how stable the folded G4s are under *in vivo* conditions and on the cell types/cycles.[5,83,84] Indeed, the folded G4 structures in the chromatin is fewer than the predicted number of G4 forming sequences,[4] implying folding of G4s might be constrained and suppressed in chromatin. Besides stabilizing and binding to several G4s, the well-known G4 binder pyridostatin most strongly affects the *SRC* proto-oncogene,[64] underscoring the fact that accessibility to G4s for small molecules may also be limited.

**Specific Targeting of Promoter G4s by Small Molecules.** Pyridine, 1,8-naphthiridine, and 1,10-phenanthroline-based bisbenzimidazole carboxamide derivatives with strategically positioned flexible dimethylamino alkyl side chains were screened for their ability to stabilize telomeric and promoter G4s.[85] Various biophysical and biochemical studies were utilized to validate the specificity of these ligands for the promoter *c-MYC* and *c-KIT* G4 DNAs. The lead ligand **Phen-Et** (Figure 3) imparted higher stabilization to promoter *c-MYC* and *c-KIT* G4 DNAs (maximum $\Delta T_{1/2} \approx 20$ °C) than to any of the telomeric G4 topologies (antiparallel, parallel, hybrid, and higher-order) and duplex DNAs. NMR studies indicated that **Phen-Et** binds to G4 through end-stacking with 1:1 stoichiometry. UV−Vis titration experiments showed that ligand binds specifically ($K_d$ = 15.6 μM) to *c-MYC* G4 DNA over telomeric and duplex DNA. Molecular modeling and dynamics (MD) studies revealed that the ligand by reorienting 5′ flanking nucleotides of *c-MYC* G4 maximizes the accessible surface area for favorable stacking interactions with the G-quartet of *c-MYC* G4. Moreover, the MD studies highlighted the importance of flexible N-alkyl side chains attached to the benzimidazole-scaffold in recognizing the propeller loops of the promoter G4 DNAs in achieving the specificity.[85]

Indenopyrimidine derivative comprising a flexible side chain protruding with pyrrolidine has been reported to specifically stabilize promoter *c-MYC* and *c-KIT1* G4s as compared to their telomeric counterpart (**Inpy1** in Figure 3).[86] **Inpy1** imparts high stability (maximum $\Delta T_{1/2} \approx 9.6$ °C) to *c-MYC* and *c-KIT1* G4s over the telomeric G4 DNAs ($\Delta T_{1/2} \approx 1.5$ °C). Stern−Volmer binding constant analysis using fluorescence titrations revealed that its binding affinity for *c-MYC* G4 is 1 order of magnitude higher than that obtained for telomeric G4.[86] MD studies showed that **InPy1** stacks on both quartets and makes unique contacts with propeller loops and flanking nucleotides. Besides, a benzene ring attached to the indenopyrimidine core is also crucial for the observed target specificity.[86]

Benzothiazole hydrazones of furylbenzamides containing different side chains have been studied for their ability to interact with various G4s. The lead ligand (**BHFB-2** in Figure 3) exhibited preferential stabilization of *c-MYC* and *c-KIT1* promoter G4 DNAs over the telomeric and antiparallel *HRAS-1* G4s.[87] Aromatic moieties of **BHFB-2** stacks well on the 5′-


DOI: 10.1021/acschembio.9b00475
ACS Chem. Biol. 2019, 14, 2102−2114

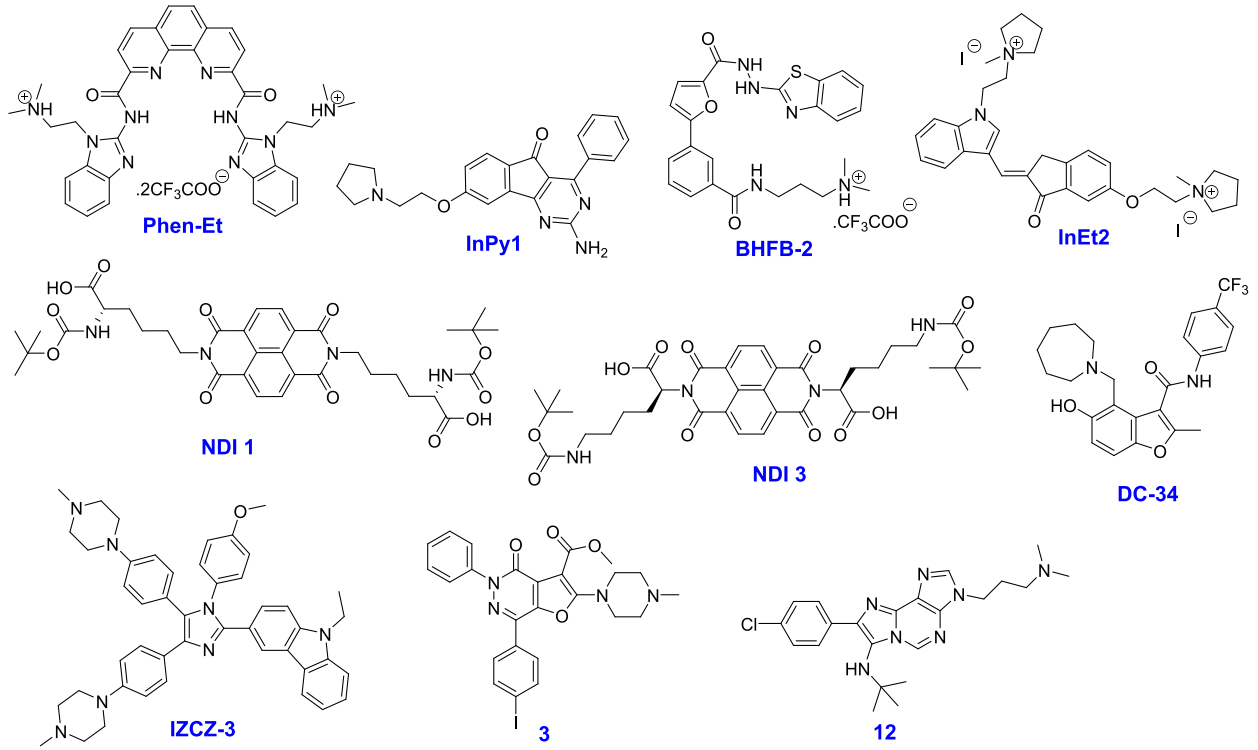


**Figure 3.** Structures of ligands that specifically stabilize promoter G4s as compared to their telomeric counterpart.

end of the G-quartets of *c-MYC* and *c-KIT1*, while the positively charged side chain involves in electrostatic interaction with a propeller loop.[87]

Indolylmethyleneindanone aromatic core with varying length of alkyl-pyrrolidine side chains was reported for their specific stabilization of parallel topology of promoter *c-MYC* and *c-KIT* G4 DNAs.[88] The lead ligand **InEt2** (Figure 3) is water-soluble and has desirable drug-like properties. It imparted high stability to *c-MYC* and *c-KIT1* and *c-KIT2* G4s ($\Delta T_{1/2}$ up to 22 °C) and did not stabilize the telomeric G4 DNA. Isothermal titration calorimetry (ITC) and electrospray ionization mass spectrometry (ESI-MS) experiments indicated that **InEt2** binds ($K_d \approx 1-10$ $\mu$M) to promoter G4 with 2:1 stoichiometry (**InEt2**/G4).[88] Molecular modeling and dynamics studies demonstrated both the 5′- and 3′-ends of G-quartets are the binding sites for **InEt2**.[88]

Several derivatives of naphthalenediimides (NDIs) have been explored as G4 stabilizing agents.[54,72] Interestingly, the recently reported amino acid functionalized NDIs exhibited specific stabilization of promoter G4 as compared to telomeric G4.[89] Notably, **NDI 1** (Figure 3) imparted stability to both *c-KIT2* and *c-MYC*, while **NDI 3** was even able to distinguish *c-KIT2* ($\Delta T_{1/2}$ = 14.6 °C) from *c-MYC* ($\Delta T_{1/2}$ = 0.1 °C).[89] On the one hand, this study highlights the profound effect of the amino acid side chains in differentiating two closely related promoter G4s. On the other hand, the role of the unusual *t*-butyloxycarbonyl (BOC) group in the side chains remains to be elucidated.

Attachment of carbazole moiety into a triaryl-substituted imidazole resulted in a four-leaf cloverlike ligand **IZCZ-3** (Figure 3).[90] Fluorescence studies indicate that ligand binds to *c-MYC* G4 with 1:1 stoichiometry and a $K_d$ of ∼0.1 $\mu$M. The thermal melting analysis showed that **IZCZ-3** imparted high thermal stability to *c-MYC* G4 ($\Delta T_{1/2}$ = 20 °C) and had little effect on other G4s from telomeric, *HRAS*, *c-KIT1*, *BCL-2*, and *KRAS*, highlighting specific stabilization to *c-MYC* G4.[90] Cellular studies indicated that the ligand effectively downregulates *c-MYC* transcription and inhibits cancer cell growth. It also inhibits cervical squamous cancer growth in mouse xenograft models.[90]

Small molecule microarray screening of 20 000 molecules led to the identification one drug-like small molecule capable of binding to *c-MYC* G4 selectively.[91] Further optimization resulted in **DC-34** (Figure 3) that binds to *c-MYC* G4 with a $K_d$ of 3.5 $\mu$M.[92] The structure−activity relationship of **DC-34** indicated that electron-withdrawing $CF_3$ group at para position on the benzene ring and azepane ring are crucial in maintaining its affinity and ability to suppress *MYC* expression. The molecule specifically stabilizes *c-MYC* G4 over several other G4s derived from *KRAS*, *MYB*, *HIF1*, and telomeric region.[92] Gene expression analysis measured by quantitative polymerase chain reaction (qPCR) indicated that **DC-34** substantially downregulats the *MYC* RNA level as compared to other G4 forming genes. Detailed structural analysis of ligand-G4 complex revealed that **DC-34** binds at both 5′ and 3′ end quartets, forming 2:1 complex using stacking, hydrogen bonding, and cation-$\pi$ interactions (Figure 4).[92] The oxygen atom from benzofuran and fluorines from trifluoromethyl group were involved in hydrogen bonding with the nucleobases of the receptor (Figure 4C). Because of its short loops and flexible flanking sequences, *c-MYC* G4 provides the more accessible binding pocket for **DC-34**, thereby providing specificity over *KRAS* and *BCL-2* G4s.[92]

Furopyridazinone-based compounds were screened to explore their ability to stabilize various G4s.[93] Results showed that the lead ligand **3** (Figure 3) binds and stabilizes the *BCL-2* G4 ($K_d \approx 1.6$ $\mu$M) specifically over other promoter and telomeric G4s, and duplex DNA.[93] Cellular assays showed that Jurkat cells treated with **3** downregulated *BCL-2* mRNA level and its protein expression significantly, validating the


DOI: 10.1021/acschembio.9b00475
ACS Chem. Biol. 2019, 14, 2102−2114

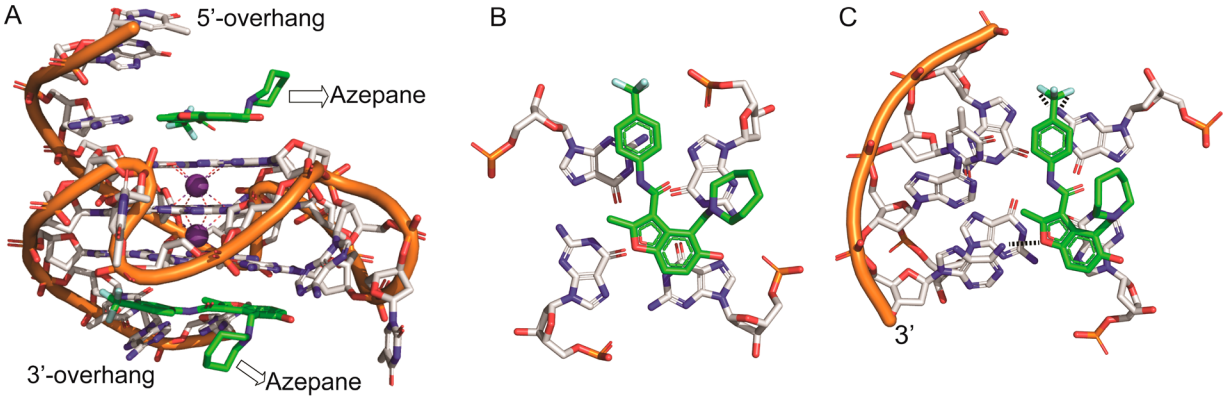


**Figure 4.** Structure of *c-MYC* G4 with ligand **DC-34** (structure shown in Figure 3), derived from NMR (PDB: 5W77).[92] $K^+$ ions are shown in purple sphere; the strand backbone and nucleosides are represented in cartoon and stick model. (A) The 2:1 (ligand/G4) complex showing $\pi-\pi$ interaction between the ligand and top as well as bottom quartet (side view). While benzofuran and *para*-trifluoromethylbenzene rings of DC-34 are involved in stacking interactions, the azepane ring is directed away from the quartet. (B) Ligand stacks on the 5′-quartet (axial view). (C) Ligand stacks on the 3′-quartet shown in axial view. The 3′-quartet includes the flanking nucleotides; the hydrogen bonds between the ligand and nucleobases are shown in dotted line. Figures are rendered using PyMOL.

biophysical assays.[93] Given the limited number of small molecules, reported to date, have drug-like properties, the furopyridazinone core is highly desired for further derivatization toward the development of G4 specific ligands.

To develop G4-ligands with drug-like properties, recently, a bioinspired approach was adopted wherein nucleobase-based scaffolds were initially screened against various G4s.[94] Initial screening based on CD melting led to the identification of a lead compound that stabilizes promoter G4s over telomeric and hairpin-duplex DNA.[94] Subsequent screening of analogues rendered compounds including **12** (Figure 3), which is found to be highly specific to *BCL-2* and *c-MYC* G4s. Compound **12** binds to *c-MYC* ($K_d \approx 26\ \mu M$) and *BCL-2* ($K_d \approx 60\ \mu M$) and represses their expression levels of the mRNA and protein.[94] Binding analysis indicated that **12** stacks on 5′-quartet of *c-MYC*, whereas it binds to 3′-quartet in case of *BCL-2*. Compound **12** has the potential to become a G4-based therapeutic agent due to its desirable drug-like properties such as having low molecular weight, water solubility, and nontoxicity.[94]

**Fluorescent Probes Specifically Recognizing Promoter G4s.** Various commercially available probes such as thiazole orange (**TO**),[95] thioflavin T (**ThT**),[96] and *N*-methyl mesoporphyrin IX (**NMM**)[97] have been utilized as G4 sensing probes and in ligand-screening assays. Besides, various synthetic probes[98] have been developed to visualize the G4s *in vitro* as well as in cellular environment.[7,99,100] G4s offer ideal hydrophobic microenvironment for fluorophores to bind, which induce various structural effects in the fluorophores such as planarity, rigidity, hydrophobicity, and monomer formation (from aggregates) upon photoexcitation, thereby resulting in their fluoresce light-up.[96,101] Several smart G4 specific fluorescent probes are currently being developed by systematic screening against various G4s. Here the probes (Figure 5) that distinguish promoter G4s from other G4s are discussed.

Replacement of one pyridine ring in 3,6-bis(1-methyl-4-vinylpyridinium) carbazole diiodide (**BMVC**)[102] by a benzindole moiety and other modifications rendered a fluorescent probe **9E PBIC** (Figure 5, Table 1) with a longer emission wavelength.[103] On the one hand, **9E PBIC** specifically enhanced its fluorescence over 100-fold in the presence of *c-MYC* G4, compared to 30-fold enhancement observed in the presence of other promoter and telomeric G4s. On the other hand, only a marginal fluorescence enhancement was observed with other nucleic acids. **9E PBIC** binds to *c-MYC* G4 ($K_d \approx 10\ \mu M$) via an end-stacking mode with 1:1 stoichiometry.[103]

**Carbazole TO** (Figure 5, Table 1) specifically enhanced its fluorescence over 70-fold in the presence of *BCL-2* G4 as compared to less than 30-fold observed with promoter (*c-MYC*, *c-KIT1*, and *VEGF*) and telomeric G4s and other nucleic acids.[104] In addition, **Carbazole TO** is able to detect *BCL-2* G4 down to 0.6 nM concentration. The quasi-planar conformation of **Carbazole TO** stacks effectively on the G-quartet of the *BCL-2* G4, with a $K_d$ of ∼2.9 $\mu$M.[104] Detailed structural studies are warranted to elucidate the role of the carboxylic acid side chain in the G4 recognition.

An acetylene-bridged 6,8-purine dimer (**APD** in Figure 5, Table 1) was reported as a selective fluorescent probe for various parallel G4 DNAs (*c-MYC*, *c-KIT1*, *c-SRC1*) and RNAs (*BCL-2*, *NRAS*, TERRA) over antiparallel promoter and telomeric G4s.[105] The **APD** dye selectively stains parallel G4 DNAs and RNAs over duplex and telomeric G4 DNAs in agarose gels. The marked fluorescence enhancement in the presence of parallel G4s was ascribed to the change in rotational diffusion of acetylene bond upon binding G4s via end-stacking.[105] Though selectivity between parallel promoter G4s and RNA G4s remains to be addressed, this core structure provides an opportunity for further molecular tweaking to make it specific to parallel promoter G4s. Although parallel G4s exist among telomeric DNA, several promoter DNAs, UTR RNAs, and telomeric RNA, the propeller loops present in them are distinct. For example, parallel telomeric G4 contains 3-nt long propeller loops, whereas *c-MYC* has short (two 1-nt and one 2-nt loops) propeller loops (Figure 1). In case of RNA G4s, they have 2′-hydroxyl functional groups. These subtle structural variations and the additional 2′-hydroxyl groups could be used to design probes for parallel promoter G4s.

Derivatives of 2,4,5-triaryl-substituted imidazole are known to display parallel G4-specific fluorescence enhancement.[106,116,117] Target(G4)-guided synthesis involving triarylimidazole containing alkyne group as the binding substrate and various azide compounds as side chains followed by *in situ*



DOI: 10.1021/acschembio.9b00475
ACS Chem. Biol. 2019, 14, 2102−2114

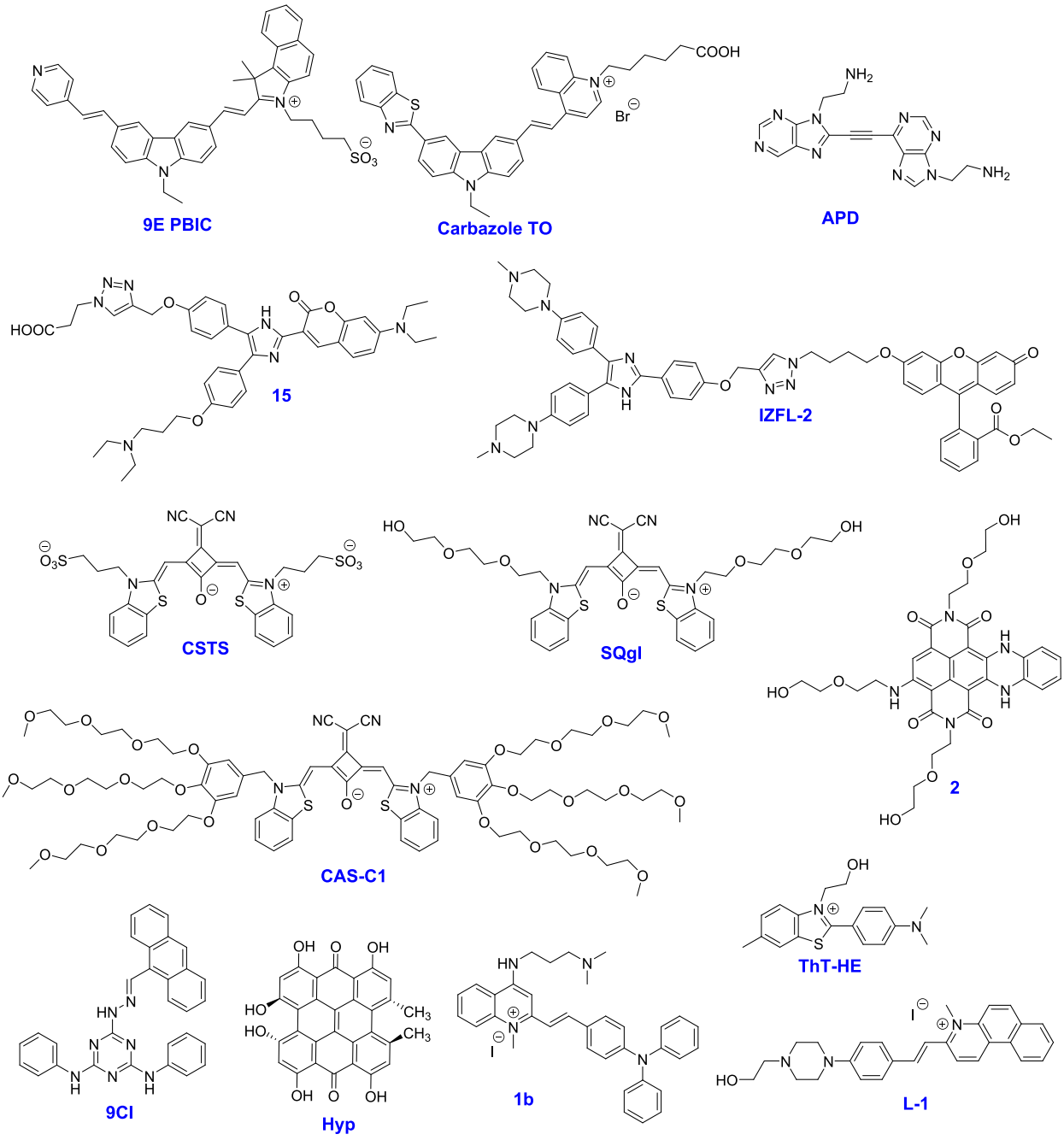


**Figure 5.** Structures of molecules that light-up fluorescence upon binding to promoter G4 structures.

click chemistry resulted in the formation of compound **15** (Figure 5, Table 1),[106] which displayed a marked fluorescence enhancement upon binding to *KRAS*, *c-MYC*, *c-KIT2*, and *BCL-2* G4s, whereas it weakly fluoresced in the presence of *HRAS*, telomeric G4, and other nucleic acids.[106] Compound **15** was also used as a specific staining agent for parallel G4s in the gel.[106]

A smart fluorescent probe **IZFL-2** (Figure 5, Table 1) was designed by harnessing the photoinduced electron transfer (PeT) mechanism.[107] The PeT-based probe was rationally constructed by attaching the fluorescein moiety to the triarylimidazole moiety (a G4 ligand) through an appropriate linker.[107] Fluorescence studies on **IZFL-2** and various G4s showed a distinct response for *c-MYC* G4. Among all the tested G4s that include telomeric, *c-MYC*, *c-KIT1*, *c-KIT2*, *BCL-2*, *KRAS*, *VEGF*, etc., **IZFL-2** exhibits a fluorescence enhancement (>10-fold) only in the presence of *c-MYC* G4, indicating its exquisite specificity to a particular G4 structure. Upon binding to *c-MYC* G4, **IZFL-2** suppresses the intramolecular PeT process, thereby restoring its fluorescence.[107] This smart probe is one of the very few probes that recognize one particular G4 among other structurally similar promoter G4s.

Many squaraine-based molecules exhibit specific recognition of promoter G4s as compared to their telomeric counterpart.[101,108,109,118] A dicyanomethylene-functionalized squarine dye with bisbenzothiazole was reported (**CSTS** in Figure 5, Table 1) as a selective probe for parallel G4s.[101] The presence of dicyanomethylene group on the central squaraine forces **CSTS** to be a crescent-shaped cisoid conformation due to steric congestion.[101] **CSTS** self-aggregates and thus exists in



DOI: 10.1021/acschembio.9b00475
ACS Chem. Biol. 2019, 14, 2102−2114

**Table 1. Promoter G4 Selective Fluorescent Probes (Figure 5) with Their Excitation and Emission Wavelengths**

| fluorescent probes | $\lambda_{ex}$ and $\lambda_{em}$ (nm) | exhibited selectivity | refs |
|---|---|---|---|
| **9E-PBIC** | 530, ∼600 | *c-MYC* | 103 |
| **Carbazole TO** | 500, 605 | *BCL-2* | 104 |
| **APD** | 430, 510 | *c-SRC1*, *c-KIT1*, RNA G4s | 105 |
| **15** | 450, 525 | *KRAS*, *c-MYC*, *c-KIT2*, *BCL-2* | 106 |
| **IZFL-2** | 450, 520 | *c-MYC* | 107 |
| **CSTS** | 680, 710 | *c-MYC*, *c-KIT2* | 101 |
| **SQgI** | 661, 700 | *VEGF*, *CEB25*, *VAV-1*, *c-MYC* | 108 |
| **CAS-C1** | 699, 719−722 | *VAV-1*, *c-MYC*, *BCL-2*, *KRARS*, *CEB25*, *VEGF* | 109 |
| **2** | 650, 685−695 | *CEB25*, *c-MYC*, *BCL-2* | 110 |
| **ThT-HE** | 415, 485 | *c-MYC* | 111 |
| **9CI** | 405, 472 | *c-MYC* | 112 |
| **Hyp** | 555, ∼610 | *c-MYC*, *c-KIT2* | 113 |
| **1b** | 470, 595 | HRAS | 114 |
| **L-1** | 463, 590 | *c-MYC* | 115 |

the H-aggregate form (nonfluorescent) in an aqueous solution. However, it disassembles and converts into the monomeric form in the presence of parallel G4s such as *c-MYC* and *c-KIT2*, thereby enhancing its fluorescence.[101] Fluorescence studies with other G4 topologies including telomeric DNA indicated that it specifically recognizes the parallel G4s over mixed-type and antiparallel ones.[101]

To overcome the low fluorescence light-up observed with **CSTS**, anamphiphilic squaraine derivative with two triethylene glycol chains (**SQgI** in Figure 5, Table 1) was reported.[108] **SQgI** enhanced its fluorescence light-up by 20 000-fold in the presence of various promoter G4s such as *VAV-1*, *BCL-2*, *VEGF*, *c-MYC*, etc. as compared to the low-level light-up observed with telomeric G4 and other nucleic acids. **SQgI** forms a sandwich-type complex (**SQgI**/G4, 1:2) with promoter G4, while the triethylene glycol side chains interact with the propeller loops through hydrogen-bonding interactions.[108] Further optimization of **SQgI** led to the development of a superior probe (**CAS-C1** in Figure 5) with improved water solubility, enhanced binding affinity, and red-shifted excitation wavelength (720 nm in the near-infrared (NIR) region).[109] The **CAS-C1** comprises six triethylene glycol chains that improve its water solubility and also strengthen the noncovalent interactions with the residues in the grooves.[109] Dissociation constants of **CAS-C1** for various promoter G4s (e.g., ∼100 nM for *c-MYC*) were found to be 2 orders of magnitude less than those of **SQgI** (∼8.3 $\mu$M for *c-MYC*). The observed specificity toward parallel G4s was ascribed to the fact that the G-quartet surface areas of parallel G4s are highly accessible for squaraine core to stack, as they are devoid of diagonal and lateral loops.[109] Moreover, **CAS-C1**-parallel G4 systems exhibit high fluorescence quantum yields and large two-photon absorption cross sections, making **CAS-C1** an ideal probe for *in vivo* applications.

Thioflavin T (**ThT**) is a selective fluorescence sensor for various G4 nucleic acids.[96,119,120] It also elicits its fluorescence response upon binding to the G4 RNA aptamer (Corn).[121] To distinguish one G4 from others, the methyl group present at N3 position on the benzothiazole ring of **ThT** was modified into a hydroxyethyl group (**ThT-HE** in Figure 5, Table 1).[111] Fluorescence studies indicated that **ThT-HE** strongly fluoresced (up to ∼240-fold) in the presence of *c-MYC* (27-mer) G4, whereas it weakly fluoresced in presence ofother nucleic acids such as telomeric and other promoter G4s, single-strand DNA (ss-DNA), and double-strand DNA (ds-DNA).[111] Overall, **ThT-HE** can address the issues such as G4 specificity and fluorescence sensitivity associated with the **ThT**.

On the one hand, the core-extended naphthalenediimide comprising three diethylene glycols (**2** in Figure 5, Table 1) as side chains exhibited high fluorescence light-up (up to ∼250-fold) in the presence of several parallel G4s of the minisatellite (CEB25), *c-MYC*, *BCL-2* etc.[110] On the other hand, it displayed a moderate fluorescence response in the presence of other nonparallel G4s. Compound **2** was able to specifically stain parallel G4s in gels.[110] The study also highlights the role of diethylene glycol side chains in achieving specific recognition of parallel G4s.

Structure-based virtual screening and subsequent lead optimization resulted in a specific fluorescent probe containing anthracene attached to a triazine derivative (**9CI** in Figure 5).[112] Fluorescence studies showed that **9CI** recognizes the *c-MYC* G4 with high specificity over other promoter G4s (*c-KIT1*, *c-KIT2*, *VEGF*, *KRAS*, etc.), human telomeric G4, and non-G4 forming sequences.[112] In addition, **9CI** was able to specifically stain *c-MYC* G4 over other nucleic acids in gel-based assay and was able to detect *c-MYC* G4 as low as 3 nM. One of the potential applications of **9CI** includes visualization of aptamer−protein binding interactions.[112]

Fluorescence studies on hypericin (**Hyp** in Figure 5, Table 1), which is one of the main components of Saint John's wort (*Hypercium*), with various nucleic acids pointed out its preference for the *c-KIT2* and *c-MYC* G4s over telomeric G4 and single-stranded and duplex DNAs.[113] On the one hand, the **Hyp** exists in aggregated forms in the aqueous environment, owing to hydrophobic interactions and hydrogen bonding.[113] On the other hand, formation of the monomeric forms contributes to its fluorescence light-up behavior in the presence of *c-KIT2* and *c-MYC* G4 DNAs.[113] Binding mode analyses by NMR, docking, and G4/hemin peroxidase inhibition studies indicated that **Hyp** stacks onto the top quartet of the parallel G4s.[113]

Triphenylamine-quinolinium derivative with 2-(dimethylamino)ethyl amino group as a side chain was reported as a selective G4 fluorescent probe.[122] Further optimization with the side chain length into the 3-(dimethylamino)propyl amino group resulted in probe **1b** (Figure 5, Table 1), which is highly selective for *HRAS* G4 (antiparallel form) over other promoter and telomeric G4s.[114] **1b** exhibited more than 180-fold emission enhancement in the presence of *HRAS* G4. Further, **1b** could be used to detect *HRAS* G4 with a limit of detection ∼1.12 nM. Interestingly, **1b** was found to be cell-permeable and provided a red signal in nucleoli, demonstrating its potential application in live-cell imaging.[114] This study highlights the critical role of length of the amine side chain in distinguishing *HRAS* G4 over other G4 structures.

A fluorescent probe based on benzo[*f*]quinolinium derivative with styryl moiety was reported for selective recognition of *c-MYC* G4 (**L-1**, Figure 5, Table 1).[115] The probe exhibited red emission and a large stock shift in the presence of *c-MYC* G4. Fluorescence studies with other nucleic acid indicated that **L-1** enhanced its fluorescence by 550-fold in the presence of *c-MYC* G4. In contrast, it exhibited a moderate fluorescence enhancement (up to 310-fold) in the presence of other G4s


DOI: 10.1021/acschembio.9b00475
ACS Chem. Biol. 2019, 14, 2102−2114

and a low enhancement (up to 110-fold) with other nucleic acids.[115] Molecular docking study showed that the −OH group in the *N*-(2-hydroxyethyl)piperazine side chain involved in the hydrogen bonding with the negatively charged phosphate backbone of the *c-MYC* G4. Further, the side chain was found to be critical in sensing *c-MYC* G4, as the replacement of the hydroxyethyl by phenyl group resulted in the loss of fluorescnce emission.[115] Moreover, **L-1** is cell permeable and able to localize inside the nucleus, thus showing its live-cell imaging application.

## SUMMARY AND OUTLOOK

Overall, the ligands (Figures 3 and 5) can specifically or preferentially recognize promoter G4s over the telomeric and duplex DNAs, which was once considered to be an insurmountable task. Given that the limited structural details available for the G4-ligand complexes on G4 discriminating ligands, and most of the G4-specific ligands reported, are results of serendipitous findings, it is difficult to come up with the general structural features for the rational design of promoter-specific ligands. The reason on why some ligands recognize a particular G4 structure remains an outstanding question. Structural studies are warranted to understand how the functional groups in the ligands are involved in the recognition of unique loops of a particular G4 structure. The limited structural and molecular modeling studies indicate that G4-specific ligands access the available surface area on the G-quartets and maximize the $\pi-\pi$ stacking by reorienting the flexible flanking sequences at the 5′- or 3′-ends. This is likely to be facilitated by the other additive and cooperative functional contacts by the side chains of ligands with the unique accessible loops.

The limited success achieved in the past few years provides some hints for the design of specific ligands. For example, the central core of the well-known G4 stabilizing agents should be considered as leads, to which varying lengths of flexible alkyl side chains containing functional groups (-N- and -O-based) are to be strategically attached so as to target unique loops, as reported for **Phen-Et**, **NDI 1**, **NDI 3**, **1b**, and **ThT-HE** (Figures 3 and 5). Additionally, the number, length, and position of the side chains are likely to play a crucial role in making the ligands topology-specific.

High-throughput methods help screen the vast chemical space of drug-like small molecules. In this direction, the small-molecule microarray screening method is promising, as it allows one to screen thousands of molecules in a single set of experiments.[91] Prior to the intended screening with the G4 of interest, depleting number of small molecules that bind to the other related G4s and other nucleic acids will aid in identifying G4 specific ligands. Further, the target-guided synthesis approach[123] has also the potential to find the small molecules capable of binding to a specific G4. For example, one can exclude the nonspecific ligands from the library by incorporating appropriate control experiments with unintended G4 targets before performing screening with the intended target.

The success in the development of smart probe (**IZFL-2** in Figure 5) implies that G4-specific ligands could judiciously be assembled with appropriate fluorophores and linkers by utilizing PeT process. Moreover, the presence of triaryl-substituted imidazole core in **IZCZ-3** (Figure 3), **15**, and **IZFL-2** (Figure 5) indicates its pivotal role in interacting with promoter G4. Thus, exploring chemical space around this central core will potentially result in novel small molecules with specific binding toward a particular promoter G4 structure.

It also appears that there exists a fine tradeoff between binding affinity and specificity.[110] Many of the universal G4 stabilizing and binding agents such as pyridostatin and BRACO-19 have their $K_d$ in the nanomolar range (∼390 nM for pyridostatin and ∼33 nM for BRACO-19),[124,125] whereas all the G4-specific ligands (Figure 3) and most of the fluorescent probes (Figure 5) have their $K_d$ in the micromolar range. On the one hand, these results indicate that highly potent G4 binding ligands are likely to bind all G4s promiscuously with little or no discrimination. On the other hand, G4-specific ligands and probes uphold their biding specificity toward their cognate G4s but with moderate binding affinity. Recently, RNA aptamers named Spinach,[126] Broccoli,[127] Corn,[128] and Chili[129] that bind to GFP chromophore analogues and those named Mango (I to IV)[130−132] that bind to thiazole orange derivatives have been discovered by *in vitro* selections or reselections or reengineering. Intriguingly, these aptamers contain G4 structures, whose G-quartets are binding sites for the fluorophores.[132−135]Given their demonstrated applications in imaging cellular RNAs, the fluorophores offer an opportunity to explore chemical space around them for the development of G4-specific probes for cellular applications.

The presence of hydroxyethyl and poly(ethylene glycol) groups in **ThT-HE**, **L-1**, **SQgI**, **CAS-C1**, and **2** (Figure 5) suggests that they could be exploited as side chains when designing parallel G4 specific ligands, which potentially reduce the nonspecific interactions between the positively charged amine side chains in the ligands and negatively charged phosphate backbone in the receptor G4s.[110] Moreover, the oligoethylene glycols, containing hydrocarbons, ether groups, and hydroxyl groups, can interact with G4 nucleic acids through lone-pair$-\pi$ and CH$-\pi$ interactions, besides the hydrogen bonding.[136] Therefore, ligands with oligoethylene glycols are more likely to result in specific interactions with the receptor G4s.

The rational design of G4 ligands reported mostly considered noncovalent interactions such as stacking, hydrogen bonding, and electrostatic interaction to achieve target recognition. Intriguingly, the negatively charged side chains (carboxylic or sulfonic acid groups) present in **NDI 1**, **NDI 3**, **Carbazole TO**, **9E BPIC**, **15**, **CSTS** (Figures 3 and 5) hint that they can also be used for the development of structure-specific fluorescent probes, albeit their role remains unclear besides improving water solubility. Further, the presence of hydrophobic *t*-butyl groups in **NDI-1**, **NDI-3**, and **12** (Figure 3) implies that other noncovalent interactions are likely to play to key roles in recognizing a particular promoter G4 topology.

The selectivity of most of the probes (Figure 5 and Table 1) needs to be improved. As the field is burgeoning, advances in the molecular engineering will likely result in next-generation probes with superior selectivity toward the targeted G4 over others. Overall, the quest for the G4-specific ligands and probes is being actively pursued, and this will bring out novel drug-like small molecules and smart fluorescent probes, which in turn may find applications in G4-based therapeutics, diagnostics, and sensing.

## AUTHOR INFORMATION

### Corresponding Authors

*E-mail: dhamodharan.venugopal@oist.jp. (V.D.)



DOI: 10.1021/acschembio.9b00475
*ACS Chem. Biol.* 2019, 14, 2102−2114

*E-mail: pradeep@chem.iitb.ac.in. (P.I.P.)

**ORCID**

V. Dhamodharan: 0000-0002-5249-8096

P. I. Pradeepkumar: 0000-0001-9104-3708

**Notes**

The authors declare no competing financial interest.

## ■ ACKNOWLEDGMENTS

This work is supported by a grant from Science and Engineering Research Board, Government of India (SERB, Grant No. EMR/2016/003268) to P.I.P. The past and present members of P.I.P's group involved in G4 research are acknowledged for their contributions, which are included in this review. Authors thank anonymous reviewers for their critical and constructive comments and apologize to researchers whose works, if any, we inadvertently missed out.

## ■ KEYWORDS

**Quadruplexes (G4s)** : Four-stranded nucleic acids consisting of two or more G-quartets formed by guanine (G)-rich sequences.

**Parallel G4s** : G4s whose all four strands orient into the same direction and in the case of intramolecular ones, the strands are further intertwined by three propeller (chain reversal) loops.

**Promoter G4s** : Quadruplexes formed from the G-tracts located at the upstream of genes.

**G4 Helicases** : Enzymes that unwind (unfold) the G4 structures.

**G4 ligands** : Ligands (small molecules) that bind to G4 nucleic acids.

**Dissociation constant ($K_d$)** : Concentration of ligand at which 50% of the G4 exists in the G4-ligand complex.

**Conformational selection** : Ligand binds to one of the preexisting G4 conformations, and consequently shifts the ensemble toward the ligand-favored conformation.

## ■ REFERENCES

(1) Phan, A. T. (2010) Human telomeric G-quadruplex: structures of DNA and RNA sequences. *FEBS J. 277*, 1107−1117.

(2) Bakalar, B., Heddi, B., Schmitt, E., Mechulam, Y., and Phan, A. T. (2019) A Minimal Sequence for Left-Handed G-Quadruplex Formation. *Angew. Chem., Int. Ed. 58*, 2331−2335.

(3) Chambers, V. S., Marsico, G., Boutell, J. M., Di Antonio, M., Smith, G. P., and Balasubramanian, S. (2015) High-throughput sequencing of DNA G-quadruplex structures in the human genome. *Nat. Biotechnol. 33*, 877.

(4) Hänsel-Hertsch, R., Beraldi, D., Lensing, S. V., Marsico, G., Zyner, K., Parry, A., Di Antonio, M., Pike, J., Kimura, H., Narita, M., Tannahill, D., and Balasubramanian, S. (2016) G-quadruplex structures mark human regulatory chromatin. *Nat. Genet. 48*, 1267.

(5) Biffi, G., Tannahill, D., McCafferty, J., and Balasubramanian, S. (2013) Quantitative visualization of DNA G-quadruplex structures in human cells. *Nat. Chem. 5*, 182.

(6) Biffi, G., Di Antonio, M., Tannahill, D., and Balasubramanian, S. (2014) Visualization and selective chemical targeting of RNA G-quadruplex structures in the cytoplasm of human cells. *Nat. Chem. 6*, 75.

(7) Laguerre, A., Hukezalie, K., Winckler, P., Katranji, F., Chanteloup, G., Pirrotta, M., Perrier-Cornet, J.-M., Wong, J. M. Y., and Monchaud, D. (2015) Visualization of RNA-Quadruplexes in Live Cells. *J. Am. Chem. Soc. 137*, 8521−8525.

(8) Zhang, S., Sun, H., Wang, L., Liu, Y., Chen, H., Li, Q., Guan, A., Liu, M., and Tang, Y. (2018) Real-time monitoring of DNA G-quadruplexes in living cells with a small-molecule fluorescent probe. *Nucleic Acids Res. 46*, 7522−7532.

(9) Henderson, A., Wu, Y., Huang, Y. C., Chavez, E. A., Platt, J., Johnson, F. B., Brosh, R. M., Sen, D., Jr, and Lansdorp, P. M. (2014) Detection of G-quadruplex DNA in mammalian cells. *Nucleic Acids Res. 42*, 860−869.

(10) Rhodes, D., and Lipps, H. J. (2015) G-quadruplexes and their regulatory roles in biology. *Nucleic Acids Res. 43*, 8627−8637.

(11) Paeschke, K., Bochman, M. L., Garcia, P. D., Cejka, P., Friedman, K. L., Kowalczykowski, S. C., and Zakian, V. A. (2013) Pif1 family helicases suppress genome instability at G-quadruplex motifs. *Nature 497*, 458.

(12) Lopes, J., Piazza, A., Bermejo, R., Kriegsman, B., Colosio, A., Teulade-Fichou, M.-P., Foiani, M., and Nicolas, A. (2011) G-quadruplex-induced instability during leading-strand replication. *EMBO J. 30*, 4033−4046.

(13) Collie, G. W., and Parkinson, G. N. (2011) The application of DNA and RNA G-quadruplexes to therapeutic medicines. *Chem. Soc. Rev. 40*, 5867−5892.

(14) Bugaut, A., and Balasubramanian, S. (2012) 5′-UTR RNA G-quadruplexes: translation regulation and targeting. *Nucleic Acids Res. 40*, 4727−4741.

(15) Beaudoin, J.-D., and Perreault, J.-P. (2013) Exploring mRNA 3′-UTR G-quadruplexes: evidence of roles in both alternative polyadenylation and mRNA shortening. *Nucleic Acids Res. 41*, 5898−5911.

(16) Al-Zeer, M. A., and Kurreck, J. (2019) Deciphering the Enigmatic Biological Functions of RNA Guanine-Quadruplex Motifs in Human Cells. *Biochemistry 58*, 305−311.

(17) Brázda, V., Hároníková, L., Liao, J., and Fojta, M. (2014) DNA and RNA Quadruplex-Binding Proteins. *Int. J. Mol. Sci. 15*, 17493.

(18) Mendoza, O., Bourdoncle, A., Boulé, J.-B., Brosh, J. R. M., and Mergny, J.-L. (2016) G-quadruplexes and helicases. *Nucleic Acids Res. 44*, 1989−2006.

(19) Parkinson, G. N., Lee, M. P. H., and Neidle, S. (2002) Crystal structure of parallel quadruplexes from human telomeric DNA. *Nature 417*, 876.

(20) Wang, Y., and Patel, D. J. (1993) Solution structure of the human telomeric repeat d[AG3(T2AG3)3] G-tetraplex. *Structure 1*, 263.

(21) Luu, K. N., Phan, A. T., Kuryavyi, V., Lacroix, L., and Patel, D. J. (2006) Structure of the Human Telomere in K+ Solution: An Intramolecular (3 + 1) G-Quadruplex Scaffold. *J. Am. Chem. Soc. 128*, 9963−9970.

(22) Dai, J., Carver, M., Punchihewa, C., Jones, R. A., and Yang, D. (2007) Structure of the Hybrid-2 type intramolecular human telomeric G-quadruplex in K+ solution: insights into structure polymorphism of the human telomeric sequence. *Nucleic Acids Res. 35*, 4927−4940.

(23) Lim, K. W., Amrane, S., Bouaziz, S., Xu, W., Mu, Y., Patel, D. J., Luu, K. N., and Phan, A. T. (2009) Structure of the Human Telomere in K+ Solution: A Stable Basket-Type G-Quadruplex with Only Two G-Tetrad Layers. *J. Am. Chem. Soc. 131*, 4301−4309.

(24) Liu, C., Zhou, B., Geng, Y., Yan Tam, D., Feng, R., Miao, H., Xu, N., Shi, X., You, Y., Hong, Y., Tang, B. Z., Kwan Lo, P., Kuryavyi, V., and Zhu, G. (2019) A chair-type G-quadruplex structure formed by a human telomeric variant DNA in K+ solution. *Chem. Sci. 10*, 218−226.

(25) Ambrus, A., Chen, D., Dai, J., Jones, R. A., and Yang, D. (2005) Solution Structure of the Biologically Relevant G-Quadruplex Element in the Human c-MYC Promoter. Implications for G-Quadruplex Stabilization. *Biochemistry 44*, 2048.

(26) Hsu, S.-T. D., Varnai, P., Bugaut, A., Reszka, A. P., Neidle, S., and Balasubramanian, S. (2009) A G-Rich Sequence within the c-kit Oncogene Promoter Forms a Parallel G-Quadruplex Having Asymmetric G-Tetrad Dynamics. *J. Am. Chem. Soc. 131*, 13399−13409.

(27) Yang, S. Y., Lejault, P., Chevrier, S., Boidot, R., Robertson, A. G., Wong, J. M. Y., and Monchaud, D. (2018) Transcriptome-wide



DOI: 10.1021/acschembio.9b00475
*ACS Chem. Biol.* 2019, 14, 2102−2114

identification of transient RNA G-quadruplexes in human cells. *Nat. Commun. 9*, 4730.
(28) Neidle, S. (2010) Human telomeric G-quadruplex: The current status of telomeric G-quadruplexes as therapeutic targets in human cancer. *FEBS J. 277*, 1118.
(29) McLuckie, K. I. E., Di Antonio, M., Zecchini, H., Xian, J., Caldas, C., Krippendorff, B. F., Tannahill, D., Lowe, C., and Balasubramanian, S. (2013) G-Quadruplex DNA as a Molecular Target for Induced Synthetic Lethality in Cancer Cells. *J. Am. Chem. Soc. 135*, 9640.
(30) Xu, H., Di Antonio, M., McKinney, S., Mathew, V., Ho, B., O'Neil, N. J., Santos, N. D., Silvester, J., Wei, V., Garcia, J., Kabeer, F., Lai, D., Soriano, P., Banáth, J., Chiu, D. S., Yap, D., Le, D. D., Ye, F. B., Zhang, A., Thu, K., Soong, J., Lin, S.-c., Tsai, A. H. C., Osako, T., Algara, T., Saunders, D. N., Wong, J., Xian, J., Bally, M. B., Brenton, J. D., Brown, G. W., Shah, S. P., Cescon, D., Mak, T. W., Caldas, C., Stirling, P. C., Hieter, P., Balasubramanian, S., and Aparicio, S. (2017) CX-5461 is a DNA G-quadruplex stabilizer with selective lethality in BRCA1/2 deficient tumours. *Nat. Commun. 8*, 14432.
(31) Neidle, S. (2016) Quadruplex Nucleic Acids as Novel Therapeutic Targets. *J. Med. Chem. 59*, 5987−6011.
(32) Simone, R., Fratta, P., Neidle, S., Parkinson, G. N., and Isaacs, A. M. (2015) G-quadruplexes: Emerging roles in neurodegenerative diseases and the non-coding transcriptome. *FEBS Lett. 589*, 1653−1668.
(33) Balasubramanian, S., Hurley, L. H., and Neidle, S. (2011) Targeting G-quadruplexes in gene promoters: a novel anticancer strategy? *Nat. Rev. Drug Discovery 10*, 261.
(34) Tlučková, K., Marušič, M., Tóthová, P., Bauer, L., Šket, P., Plavec, J., and Viglasky, V. (2013) Human Papillomavirus G-Quadruplexes. *Biochemistry 52*, 7207−7216.
(35) Anas, M., Sharma, R., Dhamodharan, V., Pradeepkumar, P. I., Manhas, A., Srivastava, K., Ahmed, S., and Kumar, N. (2017) Investigating Pharmacological Targeting of G-Quadruplexes in the Human Malaria Parasite. *Biochemistry 56*, 6691−6699.
(36) Buscaglia, R., Miller, M. C., Dean, W. L., Gray, R. D., Lane, A. N., Trent, J. O., and Chaires, J. B. (2013) Polyethylene glycol binding alters human telomere G-quadruplex structure by conformational selection. *Nucleic Acids Res. 41*, 7934.
(37) Heddi, B., and Phan, A. T. (2011) Structure of Human Telomeric DNA in Crowded Solution. *J. Am. Chem. Soc. 133*, 9824−9833.
(38) Hänsel, R., Löhr, F., Trantirek, L., and Dötsch, V. (2013) High-Resolution Insight into G-Overhang Architecture. *J. Am. Chem. Soc. 135*, 2816.
(39) Manna, S., Sarkar, D., and Srivatsan, S. G. (2018) A Dual-App Nucleoside Probe Provides Structural Insights into the Human Telomeric Overhang in Live Cells. *J. Am. Chem. Soc. 140*, 12622−12633.
(40) Bao, H.-L., Liu, H.-s., and Xu, Y. (2019) Hybrid-type and two-tetrad antiparallel telomere DNA G-quadruplex structures in living human cells. *Nucleic Acids Res. 47*, 4940−4947.
(41) Petraccone, L., Spink, C., Trent, J. O., Garbett, N. C., Mekmaysy, C. S., Giancola, C., and Chaires, J. B. (2011) Structure and Stability of Higher-Order Human Telomeric Quadruplexes. *J. Am. Chem. Soc. 133*, 20951.
(42) Rajendran, A., Nakano, S.-i., and Sugimoto, N. (2010) Molecular crowding of the cosolutes induces an intramolecular i-motif structure of triplet repeat DNA oligomers at neutral pH. *Chem. Commun. 46*, 1299−1301.
(43) Sun, D., and Hurley, L. H. (2009) The Importance of Negative Superhelicity in Inducing the Formation of G-Quadruplex and i-Motif Structures in the c-Myc Promoter: Implications for Drug Targeting and Control of Gene Expression. *J. Med. Chem. 52*, 2863−2874.
(44) Cui, Y., Kong, D., Ghimire, C., Xu, C., and Mao, H. (2016) Mutually Exclusive Formation of G-Quadruplex and i-Motif Is a General Phenomenon Governed by Steric Hindrance in Duplex DNA. *Biochemistry 55*, 2291−2299.
(45) Sutherland, C., Cui, Y., Mao, H., and Hurley, L. H. (2016) A Mechanosensor Mechanism Controls the G-Quadruplex/i-Motif Molecular Switch in the MYC Promoter NHE III1. *J. Am. Chem. Soc. 138*, 14138−14151.
(46) Siddiqui-Jain, A., Grand, C. L., Bearss, D. J., and Hurley, L. H. (2002) Direct evidence for a G-quadruplex in a promoter region and its targeting with a small molecule to repress *c-MYC* transcription. *Proc. Natl. Acad. Sci. U. S. A. 99*, 11593−11598.
(47) Brooks, T. A., and Hurley, L. H. (2010) Targeting MYC Expression through G-Quadruplexes. *Genes Cancer 1*, 641−649.
(48) Carabet, L. A., Rennie, P. S., and Cherkasov, A. (2019) Therapeutic Inhibition of Myc in Cancer. Structural Bases and Computer-Aided Drug Discovery Approaches. *Int. J. Mol. Sci. 20*, 120.
(49) Brown, R. V., Danford, F. L., Gokhale, V., Hurley, L. H., and Brooks, T. A. (2011) Demonstration that Drug-targeted Down-regulation of MYC in Non-Hodgkins Lymphoma Is Directly Mediated through the Promoter G-quadruplex. *J. Biol. Chem. 286*, 41018−41027.
(50) Boddupally, P. V. L., Hahn, S., Beman, C., De, B., Brooks, T. A., Gokhale, V., and Hurley, L. H. (2012) Anticancer Activity and Cellular Repression of c-MYC by the G-Quadruplex-Stabilizing 11-Piperazinylquindoline Is Not Dependent on Direct Targeting of the G-Quadruplex in the c-MYC Promoter. *J. Med. Chem. 55*, 6076−6086.
(51) Rankin, S., Reszka, A. P., Huppert, J., Zloh, M., Parkinson, G. N., Todd, A. K., Ladame, S., Balasubramanian, S., and Neidle, S. (2005) Putative DNA Quadruplex Formation within the Human c-kit Oncogene. *J. Am. Chem. Soc. 127*, 10584−10589.
(52) Fernando, H., Reszka, A. P., Huppert, J., Ladame, S., Rankin, S., Venkitaraman, A. R., Neidle, S., and Balasubramanian, S. (2006) A Conserved Quadruplex Motif Located in a Transcription Activation Site of the Human c-kit Oncogene. *Biochemistry 45*, 7854−7860.
(53) Ashman, L. K., and Griffith, R. (2013) Therapeutic targeting of c-KIT in cancer. *Expert Opin. Invest. Drugs 22*, 103−115.
(54) Gunaratnam, M., Swank, S., Haider, S. M., Galesa, K., Reszka, A. P., Beltran, M., Cuenca, F., Fletcher, J. A., and Neidle, S. (2009) Targeting Human Gastrointestinal Stromal Tumor Cells with a Quadruplex-Binding Small Molecule. *J. Med. Chem. 52*, 3774−3783.
(55) Chen, Y., and Yang, D. (2012) Sequence, Stability, and Structure of G-Quadruplexes and Their Interactions with Drugs. *Curr. Protoc. Nucleic Acid Chem. 50*, 17151.
(56) Agrawal, P., Hatzakis, E., Guo, K., Carver, M., and Yang, D. (2013) Solution structure of the major G-quadruplex formed in the human VEGF promoter in K+: insights into loop interactions of the parallel G-quadruplexes. *Nucleic Acids Res. 41*, 10584.
(57) Agrawal, P., Lin, C., Mathad, R. I., Carver, M., and Yang, D. (2014) The Major G-Quadruplex Formed in the Human BCL-2 Proximal Promoter Adopts a Parallel Structure with a 13-nt Loop in K + Solution. *J. Am. Chem. Soc. 136*, 1750−1753.
(58) Lim, K. W., Lacroix, L., Yue, D. J. E., Lim, J. K. C., Lim, J. M. W., and Phan, A. T. (2010) Coexistence of Two Distinct G-Quadruplex Conformations in the hTERT Promoter. *J. Am. Chem. Soc. 132*, 12331−12342.
(59) Mestre-Fos, S., Penev, P. I., Suttapitugsakul, S., Hu, M., Ito, C., Petrov, A. S., Wartell, R. M., Wu, R., and Williams, L. D. (2019) G-Quadruplexes in Human Ribosomal RNA. *J. Mol. Biol. 431*, 1940−1955.
(60) Xiao, C.-D., Shibata, T., Yamamoto, Y., and Xu, Y. (2018) An intramolecular antiparallel G-quadruplex formed by human telomere RNA. *Chem. Commun. 54*, 3944−3946.
(61) Rode, A. B., Endoh, T., and Sugimoto, N. (2016) tRNA Shifts the G-quadruplex−Hairpin Conformational Equilibrium in RNA towards the Hairpin Conformer. *Angew. Chem., Int. Ed. 55*, 14315−14319.
(62) Guo, J. U., and Bartel, D. P. (2016) RNA G-quadruplexes are globally unfolded in eukaryotic cells and depleted in bacteria. *Science 353*, No. aaf5371.
(63) Hale, T. K., Norris, G. E., Jameson, G. B., and Filichev, V. V. (2014) Helicases, G4-DNAs, and Drug Design. *ChemMedChem 9*, 2031−2034.


DOI: 10.1021/acschembio.9b00475
*ACS Chem. Biol.* 2019, 14, 2102−2114

(64) Rodriguez, R., Miller, K. M., Forment, J. V., Bradshaw, C. R., Nikan, M., Britton, S., Oelschlaegel, T., Xhemalce, B., Balasubramanian, S., and Jackson, S. P. (2012) Small-molecule-induced DNA damage identifies alternative DNA structures in human genes. *Nat. Chem. Biol. 8*, 301.
(65) Hänsel-Hertsch, R., Di Antonio, M., and Balasubramanian, S. (2017) DNA G-quadruplexes in the human genome: detection, functions and therapeutic potential. *Nat. Rev. Mol. Cell Biol. 18*, 279.
(66) Li, Q., Xiang, J. F., Yang, Q. F., Sun, H. X., Guan, A. J., and Tang, Y. L. (2013) G4LDB: a database for discovering and studying G-quadruplex ligands. *Nucleic Acids Res. 41*, No. D1115.
(67) Maji, B., and Bhattacharya, S. (2014) Advances in the molecular design of potential anticancer agents via targeting of human telomeric DNA. *Chem. Commun. 50*, 6422−6438.
(68) Dhamodharan, V., Harikrishna, S., Jagadeeswaran, C., Halder, K., and Pradeepkumar, P. I. (2012) Selective G-quadruplex DNA Stabilizing Agents Based on Bisquinolinium and Bispyridinium Derivatives of 1,8-Naphthyridine. *J. Org. Chem. 77*, 229−242.
(69) Larsen, A. F., Nielsen, M. C., and Ulven, T. (2012) Tetrasubstituted Phenanthrolines as Highly Potent, Water-Soluble, and Selective G-Quadruplex Ligands. *Chem. - Eur. J. 18*, 10892−10902.
(70) Webba da Silva, M. (2007) Geometric Formalism for DNA Quadruplex Folding. *Chem. - Eur. J. 13*, 9738.
(71) Haider, S. M., Neidle, S., and Parkinson, G. N. (2011) A structural analysis of G-quadruplex/ligand interactions. *Biochimie 93*, 1239.
(72) Hampel, S. M., Sidibe, A., Gunaratnam, M., Riou, J.-F., and Neidle, S. (2010) Tetrasubstituted naphthalene diimide ligands with selectivity for telomeric G-quadruplexes and cancer cells. *Bioorg. Med. Chem. Lett. 20*, 6459−6463.
(73) Asamitsu, S., Obata, S., Yu, Z., Bando, T., and Sugiyama, H. (2019) Recent Progress of Targeted G-Quadruplex-Preferred Ligands Toward Cancer Therapy. *Molecules 24*, 429.
(74) Asamitsu, S., Bando, T., and Sugiyama, H. (2019) Ligand Design to Acquire Specificity to Intended G-Quadruplex Structures. *Chem. - Eur. J. 25*, 417−430.
(75) Hamon, F., Largy, E., Guédin-Beaurepaire, A., Rouchon-Dagois, M., Sidibe, A., Monchaud, D., Mergny, J.-L., Riou, J.-F., Nguyen, C.-H., and Teulade-Fichou, M.-P. (2011) An Acyclic Oligoheteroaryle That Discriminates Strongly between Diverse G-Quadruplex Topologies. *Angew. Chem., Int. Ed. 50*, 8745−8749.
(76) Sabharwal, N. C., Savikhin, V., Turek-Herman, J. R., Nicoludis, J. M., Szalai, V. A., and Yatsunyk, L. A. (2014) N-methylmesoporphyrin IX fluorescence as a reporter of strand orientation in guanine quadruplexes. *FEBS J. 281*, 1726−1737.
(77) Sparapani, S., Haider, S. M., Doria, F., Gunaratnam, M., and Neidle, S. (2010) Rational Design of Acridine-Based Ligands with Selectivity for Human Telomeric Quadruplexes. *J. Am. Chem. Soc. 132*, 12263−12272.
(78) Di Leva, F. S., Zizza, P., Cingolani, C., D'Angelo, C., Pagano, B., Amato, J., Salvati, E., Sissi, C., Pinato, O., Marinelli, L., Cavalli, A., Cosconati, S., Novellino, E., Randazzo, A., and Biroccio, A. (2013) Exploring the Chemical Space of G-Quadruplex Binders: Discovery of a Novel Chemotype Targeting the Human Telomeric Sequence. *J. Med. Chem. 56*, 9646−9654.
(79) Chauhan, A., Paladhi, S., Debnath, M., Mandal, S., Das, R. N., Bhowmik, S., and Dash, J. (2014) A small molecule peptidomimetic that binds to c-KIT1 G-quadruplex and exhibits antiproliferative properties in cancer cells. *Bioorg. Med. Chem. 22*, 4422−4429.
(80) Calabrese, D. R., Zlotkowski, K., Alden, S., Hewitt, W. M., Connelly, C. M., Wilson, R. M., Gaikwad, S., Chen, L., Guha, R., Thomas, C. J., Mock, B. A., and Schneekloth, J. S., Jr. (2018) Characterization of clinically used oral antiseptics as quadruplex-binding ligands. *Nucleic Acids Res. 46*, 2722−2732.
(81) Yang, C., Hu, R., Li, Q., Li, S., Xiang, J., Guo, X., Wang, S., Zeng, Y., Li, Y., and Yang, G. (2018) Visualization of Parallel G-Quadruplexes in Cells with a Series of New Developed Bis(4-aminobenzylidene)acetone Derivatives. *ACS Omega 3*, 10487−10492.
(82) Marchetti, C., Zyner, K. G., Ohnmacht, S. A., Robson, M., Haider, S. M., Morton, J. P., Marsico, G., Vo, T., Laughlin-Toth, S., Ahmed, A. A., Di Vita, G., Pazitna, I., Gunaratnam, M., Besser, R. J., Andrade, A. C. G., Diocou, S., Pike, J. A., Tannahill, D., Pedley, R. B., Evans, T. R. J., Wilson, W. D., Balasubramanian, S., and Neidle, S. (2018) Targeting Multiple Effector Pathways in Pancreatic Ductal Adenocarcinoma with a G-Quadruplex-Binding Small Molecule. *J. Med. Chem. 61*, 2500−2517.
(83) Neidle, S. (2017) Quadruplex nucleic acids as targets for anticancer therapeutics. *Nat. Rev. Chem. 1*, 0041.
(84) Piazza, A., Adrian, M., Samazan, F., Heddi, B., Hamon, F., Serero, A., Lopes, J., Teulade Fichou, M. P., Phan, A. T., and Nicolas, A. (2015) Short loop length and high thermal stability determine genomic instability induced by G quadruplex forming minisatellites. *EMBO J. 34*, 1718−1734.
(85) Dhamodharan, V., Harikrishna, S., Bhasikuttan, A. C., and Pradeepkumar, P. I. (2015) Topology Specific Stabilization of Promoter over Telomeric G-Quadruplex DNAs by Bisbenzimidazole Carboxamide Derivatives. *ACS Chem. Biol. 10*, 821−833.
(86) Diveshkumar, K. V., Sakrikar, S., Harikrishna, S., Dhamodharan, V., and Pradeepkumar, P. I. (2014) Targeting Promoter G-Quadruplex DNAs by Indenopyrimidine-Based Ligands. *ChemMedChem 9*, 2754−2765.
(87) Pany, S. P. P., Bommisetti, P., Diveshkumar, K. V., and Pradeepkumar, P. I. (2016) Benzothiazole hydrazones of furylbenzamides preferentially stabilize c-MYC and c-KIT1 promoter G-quadruplex DNAs. *Org. Biomol. Chem. 14*, 5779−5793.
(88) Diveshkumar, K. V., Sakrikar, S., Rosu, F., Harikrishna, S., Gabelica, V., and Pradeepkumar, P. I. (2016) Specific Stabilization of c-MYC and c-KIT G-Quadruplex DNA Structures by Indolylmethyleneindanone Scaffolds. *Biochemistry 55*, 3571−3585.
(89) Răsădean, D. M., Sheng, B., Dash, J., and Pantoş, G. D. (2017) Amino-Acid-Derived Naphthalenediimides as Versatile G-Quadruplex Binders. *Chem. - Eur. J. 23*, 8491−8499.
(90) Hu, M.-H., Wang, Y.-Q., Yu, Z.-Y., Hu, L.-N., Ou, T.-M., Chen, S.-B., Huang, Z.-S., and Tan, J.-H. (2018) Discovery of a New Four-Leaf Clover-Like Ligand as a Potent c-MYC Transcription Inhibitor Specifically Targeting the Promoter G-Quadruplex. *J. Med. Chem. 61*, 2447−2459.
(91) Felsenstein, K. M., Saunders, L. B., Simmons, J. K., Leon, E., Calabrese, D. R., Zhang, S., Michalowski, A., Gareiss, P., Mock, B. A., and Schneekloth, J. S. (2016) Small Molecule Microarrays Enable the Identification of a Selective, Quadruplex-Binding Inhibitor of MYC Expression. *ACS Chem. Biol. 11*, 139−148.
(92) Calabrese, D. R., Chen, X., Leon, E. C., Gaikwad, S. M., Phyo, Z., Hewitt, W. M., Alden, S., Hilimire, T. A., He, F., Michalowski, A. M., Simmons, J. K., Saunders, L. B., Zhang, S., Connors, D., Walters, K. J., Mock, B. A., and Schneekloth, J. S. (2018) Chemical and structural studies provide a mechanistic basis for recognition of the MYC G-quadruplex. *Nat. Commun. 9*, 4229.
(93) Amato, J., Pagano, A., Capasso, D., Di Gaetano, S., Giustiniano, M., Novellino, E., Randazzo, A., and Pagano, B. (2018) Targeting the BCL2 Gene Promoter G-Quadruplex with a New Class of Furopyridazinone-Based Molecules. *ChemMedChem 13*, 406−410.
(94) Pelliccia, S., Amato, J., Capasso, D., Di Gaetano, S., Massarotti, A., Piccolo, M., Irace, C., Tron, G. C., Pagano, B., Randazzo, A., Novellino, E., and Giustiniano, M. (2019) Bio-Inspired Dual-Selective BCL-2/c-MYC G-Quadruplex Binders: Design, Synthesis, and Anticancer Activity of Drug-like Imidazo[2,1-i]purine Derivatives, *J. Med. Chem.* DOI: 10.1021/acs.jmedchem.9b00262.
(95) Monchaud, D., Allain, C., and Teulade-Fichou, M.-P. (2006) Development of a fluorescent intercalator displacement assay (G4-FID) for establishing quadruplex-DNA affinity and selectivity of putative ligands. *Bioorg. Med. Chem. Lett. 16*, 4842−4845.
(96) Mohanty, J., Barooah, N., Dhamodharan, V., Harikrishna, S., Pradeepkumar, P. I., and Bhasikuttan, A. C. (2013) Thioflavin T as an Efficient Inducer and Selective Fluorescent Sensor for the Human Telomeric G-Quadruplex DNA. *J. Am. Chem. Soc. 135*, 367.


DOI: 10.1021/acschembio.9b00475
*ACS Chem. Biol.* 2019, 14, 2102−2114

(97) Nicoludis, J. M., Barrett, S. P., Mergny, J.-L., and Yatsunyk, L. A. (2012) Interaction of human telomeric DNA with N- methyl mesoporphyrin IX. *Nucleic Acids Res. 40*, 5432−5447.
(98) Vummidi, B. R., Alzeer, J., and Luedtke, N. W. (2013) Fluorescent Probes for G-Quadruplex Structures. *ChemBioChem 14*, 540−558.
(99) Shivalingam, A., Izquierdo, M. A., Marois, A. L., Vyšniauskas, A., Suhling, K., Kuimova, M. K., and Vilar, R. (2015) The interactions between a small molecule and G-quadruplexes are visualized by fluorescence lifetime imaging microscopy. *Nat. Commun. 6*, 8178.
(100) Suseela, Y. V., Narayanaswamy, N., Pratihar, S., and Govindaraju, T. (2018) Far-red fluorescent probes for canonical and non-canonical nucleic acid structures: current progress and future implications. *Chem. Soc. Rev. 47*, 1098−1131.
(101) Jin, B., Zhang, X., Zheng, W., Liu, X., Zhou, J., Zhang, N., Wang, F., and Shangguan, D. (2014) Dicyanomethylene-Functionalized Squaraine as a Highly Selective Probe for Parallel G-Quadruplexes. *Anal. Chem. 86*, 7063−7070.
(102) Chang, C.-C., Wu, J.-Y., Chien, C.-W., Wu, W.-S., Liu, H., Kang, C.-C., Yu, L.-J., and Chang, T.-C. (2003) A Fluorescent Carbazole Derivative: High Sensitivity for Quadruplex DNA. *Anal. Chem. 75*, 6177−6183.
(103) Lin, D., Fei, X., Gu, Y., Wang, C., Tang, Y., Li, R., and Zhou, J. (2015) A benzindole substituted carbazole cyanine dye: a novel targeting fluorescent probe for parallel c-myc G-quadruplexes. *Analyst 140*, 5772−5780.
(104) Gu, Y., Lin, D., Tang, Y., Fei, X., Wang, C., Zhang, B., and Zhou, J. (2018) A light-up probe targeting for Bcl-2 2345 G-quadruplex DNA with carbazole TO. *Spectrochim. Acta, Part A 191*, 180−188.
(105) Nikan, M., Di Antonio, M., Abecassis, K., McLuckie, K., and Balasubramanian, S. (2013) An Acetylene-Bridged 6,8-Purine Dimer as a Fluorescent Switch-On Probe for Parallel G-Quadruplexes. *Angew. Chem., Int. Ed. 52*, 1428−1431.
(106) Hu, M.-H., Chen, X., Chen, S.-B., Ou, T.-M., Yao, M., Gu, L.-Q., Huang, Z.-S., and Tan, J.-H. (2015) A new application of click chemistry in situ: development of fluorescent probe for specific G-quadruplex topology. *Sci. Rep. 5*, 17202.
(107) Hu, M.-H., Zhou, J., Luo, W.-H., Chen, S.-B., Huang, Z.-S., Wu, R., and Tan, J.-H. (2019) Development of a Smart Fluorescent Sensor That Specifically Recognizes the c-MYC G-Quadruplex. *Anal. Chem. 91*, 2480−2487.
(108) Grande, V., Doria, F., Freccero, M., and Würthner, F. (2017) An Aggregating Amphiphilic Squaraine: A Light-up Probe That Discriminates Parallel G-Quadruplexes. *Angew. Chem., Int. Ed. 56*, 7520−7524.
(109) Grande, V., Shen, C.-A., Deiana, M., Dudek, M., Olesiak-Banska, J., Matczyszyn, K., and Würthner, F. (2018) Selective parallel G-quadruplex recognition by a NIR-to-NIR two-photon squaraine. *Chem. Sci. 9*, 8375−8381.
(110) Zuffo, M., Guédin, A., Leriche, E.-D., Doria, F., Pirota, V., Gabelica, V., Mergny, J.-L., and Freccero, M. (2018) More is not always better: finding the right trade-off between affinity and selectivity of a G-quadruplex ligand. *Nucleic Acids Res. 46*, No. e115.
(111) Kataoka, Y., Fujita, H., Kasahara, Y., Yoshihara, T., Tobita, S., and Kuwahara, M. (2014) Minimal Thioflavin T Modifications Improve Visual Discrimination of Guanine-Quadruplex Topologies and Alter Compound-Induced Topological Structures. *Anal. Chem. 86*, 12078−12084.
(112) Hu, Z., Zhai, Q., Wei, D., Hou, H., Deng, H., Ding, J., Li, J., Xu, S., Mohamed, H. I., Gao, C., Zhang, Y., Islam, B., Haider, S. M., Cao, C., and Lan, W. (2019) Selective recognition of c-MYC Pu22 G-quadruplex by a fluorescent probe. *Nucleic Acids Res. 47*, 2190−2204.
(113) Zhang, X., Jin, B., Zheng, W., Zhang, N., Liu, X., Bing, T., Wei, Y., Wang, F., and Shangguan, D. (2016) Interaction of hypericin with guanine-rich DNA: Preferential binding to parallel G-Quadruplexes. *Dyes Pigm. 132*, 405−411.
(114) Wang, M.-Q., Wang, Z.-Y., Yang, Y.-F., Ren, G.-Y., Liu, X.-N., Li, S., Wei, J.-W., and Zhang, L. (2017) Development of a light-up fluorescent probe for HRAS G-quadruplex DNA. *Tetrahedron Lett. 58*, 3296−3300.
(115) Wang, M.-Q., Zhang, Y., Zeng, X.-Y., Yang, H., Yang, C., Fu, R.-Y., and Li, H.-J. (2019) A benzo(f)quinolinium fused chromophore-based fluorescent probe for selective detection of c-myc G-Quadruplex DNA with a red emission and a large Stocks shift. *Dyes Pigm. 168*, 334−340.
(116) Chen, S.-B., Wu, W.-B., Hu, M.-H., Ou, T.-M., Gu, L.-Q., Tan, J.-H., and Huang, Z.-S. (2014) Discovery of a new fluorescent light-up probe specific to parallel G-quadruplexes. *Chem. Commun. 50*, 12173−12176.
(117) Hu, M.-H., Chen, S.-B., Guo, R.-J., Ou, T.-M., Huang, Z.-S., and Tan, J.-H. (2015) Development of a highly sensitive fluorescent light-up probe for G-quadruplexes. *Analyst 140*, 4616−4625.
(118) Zhang, X., Wei, Y., Bing, T., Liu, X., Zhang, N., Wang, J., He, J., Jin, B., and Shangguan, D. (2017) Development of squaraine based G-quadruplex ligands using click chemistry. *Sci. Rep. 7*, 4766.
(119) Renaud de la Faverie, A., Guédin, A., Bedrat, A., Yatsunyk, L. A., and Mergny, J.-L. (2014) Thioflavin T as a fluorescence light-up probe for G4 formation. *Nucleic Acids Res. 42*, No. e65.
(120) Xu, S., Li, Q., Xiang, J., Yang, Q., Sun, H., Guan, A., Wang, L., Liu, Y., Yu, L., Shi, Y., Chen, H., and Tang, Y. (2016) Thioflavin T as an efficient fluorescence sensor for selective recognition of RNA G-quadruplexes. *Sci. Rep. 6*, 24793.
(121) Sjekloća, L., and Ferré-D'Amaré, A. R. (2019) Binding between G Quadruplexes at the Homodimer Interface of the Corn RNA Aptamer Strongly Activates Thioflavin T Fluorescence. *Cell Chem. Biol. 26*, 1159−1168.
(122) Wang, M.-Q., Liu, S., Tang, C.-P., Raza, A., Li, S., Gao, L.-X., Sun, J., and Guo, S.-P. (2017) Flexible amine-functionalized triphenylamine derivative as a fluorescent "light-up" probe for G-quadruplex DNA. *Dyes Pigm. 136*, 78−84.
(123) Panda, D., Saha, P., Das, T., and Dash, J. (2017) Target guided synthesis using DNA nano-templates for selectively assembling a G-quadruplex binding c-MYC inhibitor. *Nat. Commun. 8*, 16103.
(124) Koirala, D., Dhakal, S., Ashbridge, B., Sannohe, Y., Rodriguez, R., Sugiyama, H., Balasubramanian, S., and Mao, H. (2011) A single-molecule platform for investigation of interactions between G-quadruplexes and small-molecule ligands. *Nat. Chem. 3*, 782.
(125) White, E. W., Tanious, F., Ismail, M. A., Reszka, A. P., Neidle, S., Boykin, D. W., and Wilson, W. D. (2007) Structure-specific recognition of quadruplex DNA by organic cations: Influence of shape, substituents and charge. *Biophys. Chem. 126*, 140−153.
(126) Paige, J. S., Wu, K. Y., and Jaffrey, S. R. (2011) RNA Mimics of Green Fluorescent Protein. *Science 333*, 642−646.
(127) Filonov, G. S., Moon, J. D., Svensen, N., and Jaffrey, S. R. (2014) Broccoli: Rapid Selection of an RNA Mimic of Green Fluorescent Protein by Fluorescence-Based Selection and Directed Evolution. *J. Am. Chem. Soc. 136*, 16299−16308.
(128) Song, W., Filonov, G. S., Kim, H., Hirsch, M., Li, X., Moon, J. D., and Jaffrey, S. R. (2017) Imaging RNA polymerase III transcription using a photostable RNA−fluorophore complex. *Nat. Chem. Biol. 13*, 1187.
(129) Steinmetzger, C., Palanisamy, N., Gore, K. R., and Höbartner, C. (2019) A Multicolor Large Stokes Shift Fluorogen-Activating RNA Aptamer with Cationic Chromophores. *Chem. - Eur. J. 25*, 1931−1935.
(130) Dolgosheina, E. V., Jeng, S. C. Y., Panchapakesan, S. S. S., Cojocaru, R., Chen, P. S. K., Wilson, P. D., Hawkins, N., Wiggins, P. A., and Unrau, P. J. (2014) RNA Mango Aptamer-Fluorophore: A Bright, High-Affinity Complex for RNA Labeling and Tracking. *ACS Chem. Biol. 9*, 2412−2420.
(131) Autour, A., Jeng, S., Cawte, A., Abdolahzadeh, A., Galli, A., Panchapakesan, S. S. S., Rueda, D., Ryckelynck, M., and Unrau, P. J. (2018) Fluorogenic RNA Mango aptamers for imaging small non-coding RNAs in mammalian cells. *Nat. Commun. 9*, 656.
(132) Trachman, R. J., Abdolahzadeh, A., Andreoni, A., Cojocaru, R., Knutson, J. R., Ryckelynck, M., Unrau, P. J., and Ferré-D'Amaré, A. R. (2018) Crystal Structures of the Mango-II RNA Aptamer Reveal


DOI: 10.1021/acschembio.9b00475
*ACS Chem. Biol.* 2019, 14, 2102−2114

Heterogeneous Fluorophore Binding and Guide Engineering of Variants with Improved Selectivity and Brightness. *Biochemistry 57*, 3544−3548.
(133) Huang, H., Suslov, N. B., Li, N.-S., Shelke, S. A., Evans, M. E., Koldobskaya, Y., Rice, P. A., and Piccirilli, J. A. (2014) A G-quadruplex−containing RNA activates fluorescence in a GFP-like fluorophore. *Nat. Chem. Biol. 10*, 686.
(134) Trachman, R. J., Iii, Demeshkina, N. A., Lau, M. W. L., Panchapakesan, S. S. S., Jeng, S. C. Y., Unrau, P. J., and Ferré-D'Amaré, A. R. (2017) Structural basis for high-affinity fluorophore binding and activation by RNA Mango. *Nat. Chem. Biol. 13*, 807.
(135) Trachman, R. J., Autour, A., Jeng, S. C. Y., Abdolahzadeh, A., Andreoni, A., Cojocaru, R., Garipov, R., Dolgosheina, E. V., Knutson, J. R., Ryckelynck, M., Unrau, P. J., and Ferré-D'Amaré, A. R. (2019) Structure and functional reselection of the Mango-III fluorogenic RNA aptamer. *Nat. Chem. Biol. 15*, 472−479.
(136) Tateishi-Karimata, H., Ohyama, T., Muraoka, T., Podbevsek, P., Wawro, A. M., Tanaka, S., Nakano, S.-i., Kinbara, K., Plavec, J., and Sugimoto, N. (2017) Newly characterized interaction stabilizes DNA structure: oligoethylene glycols stabilize G-quadruplexes CH−$\pi$ interactions. *Nucleic Acids Res. 45*, 7021−7030.



DOI: 10.1021/acschembio.9b00475
*ACS Chem. Biol.* 2019, 14, 2102−2114